Infrared and Water Sorption Studies of the Hydration Structure and Mechanism in Natural and Synthetic Melanin

ARTICLE *in* THE JOURNAL OF PHYSICAL CHEMISTRY B · JULY 2010

Impact Factor: 3.3 · DOI: 10.1021/jp101833k · Source: PubMed

Infrared and Water Sorption Studies of the Hydration Structure and Mechanism in Natural and Synthetic Melanin

Maria Grazia Bridelli* and Pier Raimondo Crippa

Department of Physics and CNISM, University of Parma, Viale G. P. Usberti 7/A, I43124 Parma, Italy

Received: March 01, 2010

Although water is a structural and functional determinant in melanins, a direct study of the interaction between water and melanin is still lacking and is the subject of the present work. Melanin forms in cells and organisms' colloidal particles deriving from the hierarchical aggregation of smaller subunits such as protomolecules, stacking units, and small aggregates: its functions must be interpreted in terms of solid-state and surface properties. They are strictly connected to the porosity of the particles when they interact with water and other chemicals. The structural characteristics of water sorbed in the pores are investigated by means of FTIR in the OH stretching vibration region (4000−3000 cm^{-1}) on *Sepia* and synthetic L-Dopa melanins at different and controlled hydration degrees ($a_w = 0.06$ to 0.92). Three distinct component bands are recognized in the main OH stretching band, corresponding to three distinct water populations, showing differing behavior for the two kinds of melanin and thus accounting for different molecular structures. On this basis, the historical, albeit current, model of hydration structure of melanin granules, a "strongly" and a "weakly" bound fraction, is reassessed and rediscussed.

Introduction

Melanins, the black/brown pigments widely diffuse in nature, have represented for years an enigma for biophysicists and biochemists venturing to detect their molecular structure and to relate to it their physiological role.[1] Melanins are widely diffuse in living organisms from fungi to man; in the human body they can be found in the skin, hair, eyes, brain, and liver, accumulating in pathological forms such as the melanoma. The distribution spread over visible and nonvisible regions of the body has hindered an univocal definition of their role, and different functions have been attributed to them: photoprotection, photosensitization, metal ion chelation, antibiotic, and free radical quenching.[2,3]

In humans, melanin can be divided into two predominant forms: eumelanins (black to brown pigments) and pheomelanins (red to yellow). The macromolecular structure has not yet been completely elucidated because of the number of natural systems where it is present and of the large variety of synthetic analogues that can be produced in the laboratory, starting from different precursors, or by following different in vitro procedures established in an attempt to mimic the natural melanogenesis. Moreover, the ultrastructural organization of melanin from *Sepia officinalis* has recently been elucidated, and it can be assumed to be a general model for the assembly of the pigment.[4] The study shows that the fundamental molecular unit (protomolecule) and the protomolecule assembly originate large particles the sizes of which depend on the parameters of the cellular surroundings, such as pH, temperature, concentration, and the presence of metal ions. The protomolecule structure, particularly interesting for the present work, hypothesized in a coarse shape in 1969[5] and successively reassessed and established over the years,[6−9] can be described as a graphite-like unit, formed by planar structures built from about five DHI/DHICA monomers stacked in two to three sheets. The distance between the sheets is ∼0.34 nm, as appears from the X-ray diffraction studies, whereas the lateral extent ranges between 1.5 and 2.0 nm.[5,6,8] DHI and DHICA and their various oxidized forms appear to be the basic monomeric building blocks for both natural and synthetic compounds. Many extensive reviews have been dedicated to the elucidation of the chemistry of these biopolymers.[2,3,10−12]

Their physical properties have been investigated by means of various experimental techniques with the aim of establishing an interrelationship between structure and physiological functions.[12] These studies confirm that all known physical and chemical properties are dramatically influenced by water adsorbed and, in particular, stress because the presence of water greatly influences the "solid state" properties such as threshold switching, electrical conductivity, photoconductivity, charge or polarization storage, absorption and dispersion of sound waves, and optical properties. Pioneering experimental results suggested that water retained by melanin was in two different states. "Easy water" and "hard water" were termed the different fractions, the so-called "easy water" being a water fraction that can be lost by heating the sample to 150 °C, and the "hard water" being the part retained in the inner structure of the biopolymer at temperatures >150 °C.[5] The model was, however, defective in some aspects, such as the identification of the bonding sites for H_2O molecules in the polymer or the characterization of the physical state of the two water components as solid or liquid. Recently, many fundamental aspects of water interactions with porous solids have been investigated, and the structural resemblance of melanin to these materials has suggested that they can be assumed to be model systems for a reconsideration of the water sorption by the pigment. Activated carbons may be qualitatively described as graphitic plates more or less irregularly stacked, the interstices of which constitute the pores where water can be sorbed.[13] Water filling the pores is confined to narrow geometries and displays differing behavior from that in its bulk state. The behavior of water confined in pores of carbon materials has been the subject of several experimental and theoretical studies that have inferred changes in the water density in the pore cavity depending on various factors such as the pore

* Corresponding author. E-mail: mariagrazia.bridelli@unipr.it.

10.1021/jp101833k
Published on Web 07/06/2010

radius, the presence and density of oxygenated groups on the carbon surfaces, and the external water pressure and temperature.[13−15] The confinement has the effect of modifying the average numbers of bonds among water molecules included, so that the larger pores permit water adsorption at a more or less liquid-like density, whereas in narrower pores, the extreme confinement induces the disruption of the H-bond network among H_2O molecules and reduces the water density to low vapor-like values.[16,17] As shown by the simulation analyses, in the pore-filling process, confined water at the beginning has the typical structure of vapor, the liquid state gradually developing with increasing vapor pressure, pore radius size permitting. Such a picture is valid for a simple model; however, by extending the model to complex pore geometries, effects such as molecular structure of the pore surface, pore connectivity, and pore surface hydrophobicity might influence and modulate the solvation phenomena.

Many experimental techniques have been employed in the past to investigate the state of water adsorbed on polymer surfaces. Absorption spectroscopy in the IR frequency range is one of the most sensitive among these for studying water bound to biological macromolecules, being able to monitor changes in the structural features such as changes in water spectral properties. IR spectroscopy has contributed significantly, since 1980, to the investigation of the hydration properties of melanin, both natural and synthetic; in addition, in many papers, the spectra of melanins differing in biological origins or chemical synthesis procedures have been displayed and interpreted.[7,18,19] The typical IR spectrum of melanins is dominated by the bound water absorption bands, the broad one between 3700 and 3000 cm^{-1} due to the strongly absorbing hydroxyl stretching vibrations (ν(OH)), the relatively sharp but weaker hydroxyl bending mode (δ(OH)) around 1600 cm^{-1}, and the strongly absorbing feature below 1000 cm^{-1} due to the librational modes. The dominance of the OH normal modes of water on the polymer spectrum has been considered for years to be an obstacle to chemical analysis and has hindered the application of the technique to the study of melanins of various origins: different melanins, at first sight, exhibit in fact very similar IR absorption spectra. However, an improvement in the characterization of the spectra, at least qualitatively, has been obtained by means of the refinements of the procedures of sample preparation and has allowed for structural investigations.

In the light of these considerations, the purpose of the present study is to re-examine the infrared spectra of the melanin to elucidate the molecular structure of embedding water. Water molecules are also employed as probes to investigate the hypothesized layered structure of melanin. The FTIR spectra of two melanins, a natural one from *Sepia* ink sac (*Sepia* m.) and a synthetic one from L-Dopa autoxidation (L-Dopa m.), were obtained in transmission mode on thin films deposited on CaF_2 windows and studied in the wavenumber range where OH stretching vibrations extend. The spectral amplitudes and shapes were recorded for samples prepared at different humidities, both in adsorption and in desorption (water vapor activity a_w in the range 0.06 to 0.92). The OH stretching bands were decomposed into three Gaussian components, whose frequencies were related to the hydrogen bond distances and the amplitudes with the amount of the three water fractions adsorbed to melanin, differing in structure and clustering order, following the procedure described in recent literature.[20,21]

By appropriate manipulation of the data, sorption isotherm curves were built to show the water adsorption and desorption processes governing each water population contributing to the ν(OH) spectra. The isotherm curves were fitted by means of various curve fitting theories to test for the most reliable model to best describe the systems.

TABLE 1: Saturated Salt Solutions Employed to Obtain the Controlled Activities a_w (Expressed As a Fraction) in the Box Where Melanin Films Were Equilibrated before FTIR Measurements

salt	a_w
NaOH	0.06
LiCl	0.11
$CaCl_2$	0.29
NaI	0.38
$Ca(NO)_3$	0.51
NaBr	0.58
KI	0.69
$NaNO_3$	0.74
NH_4Cl	0.79
KCl	0.84
KNO_3	0.92

Experimental Section

Materials. Natural melanin from the ink sac of *Sepia officinalis* was purchased from Sigma Chemical Company and used without further purification.

Synthetic melanin was prepared by autoxidation of L-Dopa (Fluka AG) starting from a saturated aqueous solution. The pH was raised to 9.5 by the addition of NaOH, and the solution was stirred in air for 4 days. The black material was then dialyzed for 3 days against water with frequent changes of the bath.

A small drop of the melanin suspensions (c = 40 mg/mL) was deposited on a CaF_2 window and dried under ambient conditions.

The melanin film smeared on the CaF_2 window was assembled in a home-built sample holder equipped with IR transparent CaF_2 windows together with a vessel containing the saturated salt hydrating solution to avoid any contact of the sample with the external atmosphere and to adjust to the desirable inner relative humidity. The sample was vertically positioned in such a way as to allow for transmission measurements. The box was inserted in the FTIR spectrophotometer.

We obtained the different hydration degrees of the samples by equilibrating them for 2 days directly in the inner ambient of the box over suitable hydrating saturated salt solutions put in the vessel placed into the box and assembled together with the sample, as described above. In this way, the relative humidity was made to vary in the range 6−92%. Table 1 lists the activities a_w provided in the desiccator by each salt solution and the salts employed. The change in the hydrating solution was performed in a drybox under a controlled N_2 atmosphere.

Methods. ***FTIR Measurements.*** FTIR spectra were collected with a Jasco 420 FT/IR spectrophotometer operating at a temperature close to room temperature (290−300 K) in the transmission mode within the 4000−1000 cm^{-1} range in 128 scans at a spectral resolution of 2 cm^{-1}. The spectra provide information about both the hydration of the polymer (wavenumber range: 4000−3000 cm^{-1}) and surface functionality (ν beyond 2000 cm^{-1}). From the analysis of the low wavenumber region of the spectra, we extracted qualitative information as to the possible water adsorption centers, whereas the investigation of the water content and binding was performed on the O−H stretching mode of sorbed water falling in the high wavenumber region.

A two-fold analysis was performed on the ν(OH) band for each type of melanin. First, the spectra of the samples collected by decreasing (desorption run) and increasing (adsorption run) the ambient relative humidity were compared and analyzed. Second, by assuming that the OH stretching band is due to the distribution of hydrogen bonds of variable strength over a variety of binding sites, each ν(OH) feature was resolved by means of a deconvolution procedure into three Gaussian components, whose amplitude, converted into water amount, was used to plot the sorption isotherm curves.

Origin 7.0 software was used for the absorption band deconvolution, the component peak position being found in the second derivative spectra.

Sorption Isotherms. Sorption isotherms were calculated as a plot of the amount of water adsorbed as a function of the relative humidity, directly related to the water vapor activity, a_w. In this form, they were analyzed by the methods described below. The water amount bound to melanin was deduced from the ν(OH) band amplitude after subtraction of the spectrum of the same sample preheated to 383 K for 2 h ("dry" sample). In this way, any contribution to the band of N−H and C−H stretching vibrations, occurring in the same wavenumber range investigated, was systematically eliminated. Adaptation of Beer's law was successively used to rescale the intensity of the "cleaned" ν(OH) bands, in accordance with the approach proposed in literature to study various hydrated biomaterials and biomacromolecules[22,23]

$$A(a_w) = \varepsilon \cdot c \cdot d$$

For each value of water vapor activity (a_w), $A(a_w)$ is the measured absorbance, ε is the molar absorptivity at the wavenumber ν where the absorption line peaks (for *Sepia* melanin, $\nu_{MAX} \approx 3607$ cm^{-1}; for L-Dopa melanin, $\nu_{MAX} \approx 3405$ cm^{-1}), c is the concentration of the absorbing species (mmol/cm,^{3} or, equivalent mol/L), and d is the average thickness of the absorbing species film, that is, adsorbed water, in centimeters. For water, it is possible to calculate $\varepsilon_{3600} = 1.647$ L mol^{-1} cm^{-1} and $\varepsilon_{3400} = 1.043$ L mol^{-1} cm^{-1}. By assuming the path length for the absorbing species as the film thickness (respectively, $d_{Sepia} \approx 2 \times 10^{-4}$cm and $d_{L\text{-}dopa} \approx 3 \times 10^{-3}$ cm), the water contents for each sample for each hydration degree were estimated, and the amplitudes of the Gaussian components of the ν(OH) absorption band were thus scaled.

The computed water amounts were plotted as a function of the water activity a_w to obtain couples of sorption runs (desorption−adsorption) for each Gaussian component for each sample. The desorption experiment, the first point being taken on the sample equilibrated to the highest a_w value ($a_w = 0.92$), was always performed before the adsorption one to avoid possible damage of the samples by submitting them to drastic dehydration treatments such as heating or outgassing.

Differing theoretical fitting functions were applied to the analysis of the curves.

The present study is based on two multilayer adsorption models: the BET (Brunauer, Emmett, and Teller) theory, extended to the so-called GAB (Guggenheim, Anderson, and de Boer) equation, and the Dubinin−Serpinsky (D−S) model. The fitting of the data with these equations allows for the evaluation of some useful experimental parameters that can be correlated with physical (and biophysical) properties.

We will present only a brief outline of some equations that can be found and have been discussed in texts such as the classical book by Gregg and Sing[24] and in recent papers.[25,26]

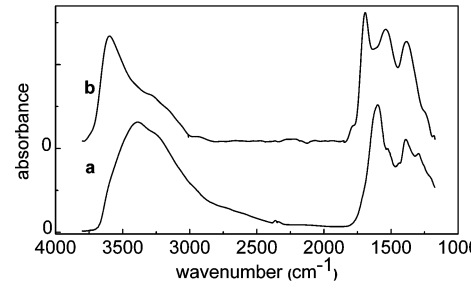

Figure 1. FTIR spectra of melanins of differing origins (a) synthetic by auto-oxidation of L-Dopa and (b) natural from *Sepia* ink sac (SIGMA). To facilitate the comparison, the *Sepia* melanin spectrum has been magnified by a factor of 2.3.

The choice of the D−S model is based on the discussion of the various theories recently reviewed by Rutherford,[27] who has evidenced that it is able to represent Henry's law at low pressures and can well describe type III isotherms.

The wel1-known BET equation can be written in the form

$$n = \frac{n_m c(P/P_0)}{[1 - (P/P_0)][1 + c(P/P_0) - P/P_0]} \quad (1)$$

With the introduction of an extra parameter, the obtained GAB equation allows for the fitting to be extended to a wider range of relative pressure values

$$n = \frac{n_m ck(P/P_0)}{[1 + k(P/P_0)][1 + ck(P/P_0) - k(P/P_0)]} \quad (2)$$

The D−S equation was used in the simplified form[26]

$$n = \frac{n_m j(P/P_0)}{1 - j(P/P_0)} \quad (3)$$

In all of the above formulas, the meaning of the terms is the following: n is the moisture content (mmol$\cdot$g^{-1}) as a function of the relative vapor pressure P/P_0, n_m is the monolayer capacity (in the D−S model it corresponds to the surface concentration of the primary hydrophilic adsorption centers, see below), and c represents a thermodynamic parameter.[24] The GAB constant k is related to the difference in the energy of adsorption between the first layers and the bulk water.

The kinetic best-fit parameter is $j = k_2/k_1$ (eq 3).

Results

FTIR Measurements. In Figure 1, FTIR spectra of L-Dopa synthetic melanin (a) and *Sepia* melanin (b) films, prepared at the highest attained activity ($a_w = 0.92$) and recorded in the wavenumber range 4000−1000 cm^{-1}, are displayed and compared.

Although the spectra of the two melanins have already been shown and discussed in several papers in the past,[1,2,7,18,19] the characteristic features are summarized here for the sake of clarity. The two spectra are similar in the main features, although some peculiar differences can be pointed out. As is well known, the wavenumber region below 2000 cm^{-1} gives information about the chemical composition of the two samples examined: in both melanin spectra, the C−N stretching feature occurring at 1386 cm^{-1} is characteristic of the aromatic fundamental units,

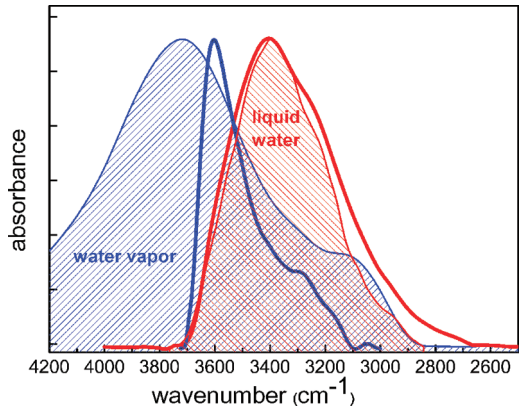

Figure 2. OH stretching bands measured for *Sepia* (solid blue curve) and L-Dopa melanin (solid red curve). We obtained the spectra by subtracting from the ν(OH) features, recorded for the samples at the highest hydration content, the spectra of the same samples dried in the oven at 383 K for 2 h. The dashed area curves represent the OH stretching bands for pure water in vapor (blue) and in liquid (red) phase taken from literature.[26] All spectra have been normalized to the maximum height peak for the sake of comparison.

that is, the pyrrole or indole ring. In *Sepia* melanin, the band is coupled to the feature at 1536 cm^{-1}, which in the synthetic one appears as the shoulder at 1524 cm^{-1}, due to indole NH bending, the shift in the absorption frequencies accounting for differences in hydrogen bonding. Significantly, the differences in the surface functional groups of the two melanins are reflected in the 1690 cm^{-1} band in the *Sepia* melanin spectrum. This is due to C═O carboxylic groups conjugated with aromatic ring, typical for quinone structures, whereas the 1600 and 1297 cm^{-1} bands in the spectrum of L-Dopa melanin can be related to the aromatic C═C and phenolic C−OH stretching, indicating a prevalence of dihydroxyindole moieties in the synthetic sample compared with the natural one.

The absorption bands arising from the hydroxyl stretching vibrations ν(OH) (wavenumber range 4000−3000 cm^{-1}) were the focus of our attention. They exhibit different shapes and amplitudes for the two melanins.

In Figure 2, the ν(OH) bands were isolated, subtracted from the spectrum of the dry samples, and plotted by normalizing the peak height to the maximum amplitude. They represent the OH stretching vibration spectra only of the water bound to the samples, as described in the Materials and Methods sections. The different amplitude of the spectra after normalization can be solely attributed to the difference in the water content, the detected disproportion suggesting that L-Dopa melanin is able to soak an amount of water far greater than the natural one for the same a_w value. As for the shape, the ν(OH) features look like asymmetric bands displaying some notable differences in the position of the maximum and in the outline. The *Sepia* melanin spectrum shows a prominent peak centered at ∼3607 cm^{-1} and a shoulder at ∼3300 cm^{-1}, and the Dopa m. spectrum displays a broad band peaking at a lower wavenumber, $\nu \approx$ 3405 cm^{-1}, with a shoulder at ∼3200 cm^{-1}.

In the picture, they are plotted superimposed upon the OH stretching bands of pure H_2O in liquid and in vapor phase[28] for comparison. The L-Dopa melanin ν(OH) band is significantly overlapped with the liquid water spectrum, whereas the absorption band for *Sepia* melanin is almost biphasic, displaying a partial overlay with the water vapor band and a broadening toward a lower wavenumber region where the absorption of both the water phases occurs.

Both shape and large bandwidth argue in favor of the ν(OH) features originating from a distribution of different vibrational energies for the contributing water molecules, although the truly important issue is that the comparison proposed in Figure 2 suggests that water does not exhibit the same aggregation state once it is adsorbed in the two melanins. To analyze this point better, a simplification of the model was necessary. We separated three distinct bands in each stretching vibrational feature by resolving it into three Gaussian components following the deconvolution procedure of the second derivative analysis. The method allowed for the identification of three types of water molecules bound to melanin, different in vibrational energies and each one characterized by a single H-bonding energy. The three bands were called high- (HW), medium- (MW), and low- (LW) wavenumber components.

From the vibrational frequencies corresponding to the maximum of the component peaks, the H-bond distances (H···OH lengths) were estimated,[29] and in Table 2, they are listed for both melanins studied.

The dehydration and rehydration treatments to which the samples were submitted affected amplitude, frequency, and width of the absorption bands and of each component. Because of the different behavior exhibited, the two different melanins were analyzed separately, and the properties are described below.

Sepia Melanin. Figure 3A shows the OH stretching band for the sample prepared at the highest water content ($a_w = 0.92$). The attempt to resolve the curve in overlapped component bands was achieved by accomplishing the deconvolution by means of least-squares optimization procedures into three Gaussian peaks marked by the following peak positions: HW at 3624 cm^{-1}, MW at 3550 cm^{-1}, and LW at 3350 cm^{-1}. As shown in Table 2, the corresponding H-bond distances were estimated at 0.31 nm for HW band, 0.23 nm for MW band, and 0.20 nm for LW band. Whereas the last two values are compatible with hydrogen bonding patterns in liquid water, the first one is a cutoff value. It can be attributed to H_2O single or bound in small clusters (such as dimers) as in the gas phase, whose structure oscillates between H-bonded and non-H-bonded. Some researchers, in fact, consider the hydrogen bond to be broken if the bond length is >0.31 nm.

Changes in the water content of the polymer are reflected in the amplitude and shape changes of the overall peak and, as a consequence, of the component bands. They can be easily correlated to the structural changes occurring in the polymer during the different hydration−dehydration treatments.

By decreasing the moisture content (by reducing a_w from 0.92 to 0.06), the overall absorption band amplitude decreases and the band thins out and shifts toward a lower wavenumber region. The band recorded at the end of the treatment is very different from that at the start, in shape and amplitude, and the resolution into components testifies to dramatic changes in the spectral contributions. In Figure 3B, the decomposition of the band shows not only that the intensity of each component is drastically reduced but also that the reciprocal ratios are notably changed. Moreover, all of the bands display a red shift throughout the treatment.

The desorption process was analyzed step by step, and the decrease in the component peak amplitude monitored as a function of the a_w values was obtained, as displayed in Figure 4 (full symbols). Two threshold a_w values deserve particular mention: $a_w = 0.84$ and 0.29. Crossing $a_w = 0.84$, all three of the component bands are drastically reduced so that the water amount removed from the polymer matrix, as deduced from the peak area, is ∼60% of the total water detained in the sample at the start of the process. a_w values falling between 0.51 and

TABLE 2: Hydrogen Bond Distances Estimated from the Vibrational Frequencies Following Nakamoto et al.[29]

Sepia melanin		L-Dopa melanin	
stretching frequency (cm^{-1})	bond distance (nm)	stretching frequency (cm^{-1})	bond distance (nm)
3624	0.31	3575	0.24
3550	0.23	3450	0.22
3350	0.20	3280	0.18

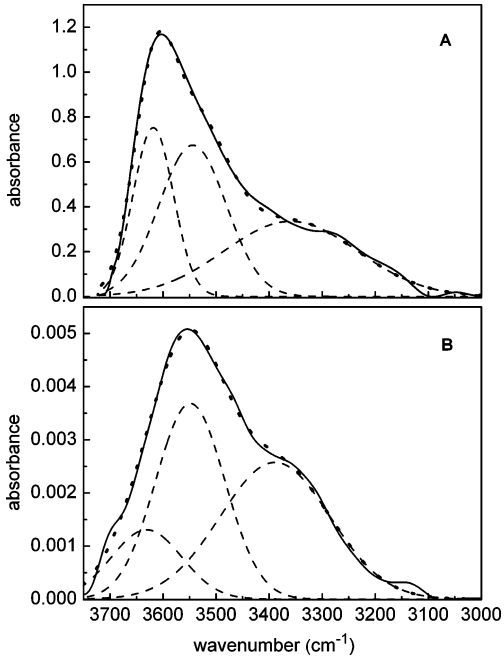

Figure 3. Gaussian deconvolution of FTIR OH stretching bands measured for *Sepia* melanin at $a_w = 0.92$ (A) and dehydrated up to $a_w = 0.06$ (B), prepared as thin films obtained by evaporation in air at room temperature of a drop of aqueous solution ($c = 40$ mg/mL). The dashed lines are the Gaussian components obtained by deconvolution of the bands. The dotted lines represent the sum of the components. They closely overlap the experimental data traces, shown as full heavy lines (goodness of fit $R = 0.997$).

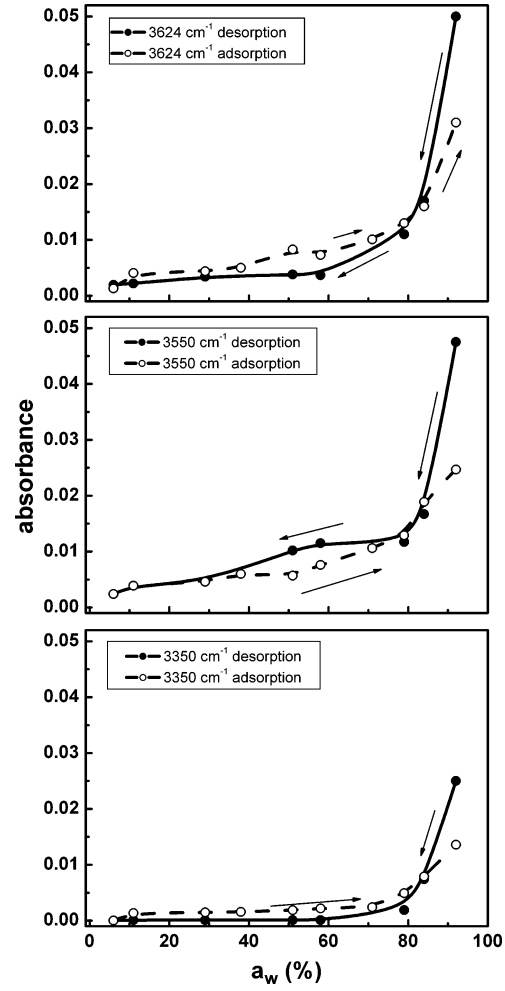

Figure 4. Desorption (●) and adsorption (○) data for *Sepia* melanin, as deduced by the amplitudes of the three ν(OH) component bands (HW, MW, and LW) during the dehydration and hydration treatments. The lines are a guide for the eye.

0.29 produce the desorption of practically all of the residual water, chiefly involving the fractions that contribute to the HW and MW components. The LW peak evolves in a simpler way: its amplitude, in fact, abruptly decreases during the first desorption step; that is, for $a_w < 0.84$, and its position shifts toward a lower wavenumber region, after which the peak, having attained a fixed position, is gradually suppressed until it practically disappears.

The kinetics of the rehydration process, performed by increasing the partial water vapor pressure from the lowest humidity level, $a_w = 0.06$, to the maximum value, $a_w = 0.92$, is recorded in Figure 4 (○). As for the HW band, the water uptake curve lies over the dehydration curve, suggesting an enhanced availability for the water in the gaseous phase of the dehydrated polymer. MW and LW bands, in contrast, seem to be unaffected by the addition of water at least up to $a_w < 0.51$, after which they begin to recover. All three of the component bands exhibit considerable hysteresis. In fact, when water is gradually returned to the sample, the overall peak increases, although it does not recover the primary amplitude, even by restoring the initial degree of hydration. In Figure 5, the two overall bands corresponding to the same hydration level ($a_w = 0.92$), one recorded at the beginning of the desorption process (curve a) and the other at the end of the adsorption run after desorption (curve b), are superimposed for comparison. The difference band (curve c) is conspicuous and can be regarded as the spectrum of the water that can no longer be drawn back into the sample after the dehydration treatment. This difference band was analyzed and decomposed into Gaussian components, as shown in the inset. Surprisingly it was impossible to resolve it into the three original components: in fact, the HW band cannot be regained. In the inset of Figure 5, the decomposition of curve c into the two residual Gaussian component bands is shown. They peak at 3580 and 3370 cm^{-1}, roughly filling the position of the original MW and LW peaks. The result emphasizes the hypothesis that a considerable liquid water portion, once desorbed, cannot be readsorbed. Its amount is ~64% of the original water content, as estimated from the area under the curves.

Synthetic L-Dopa Melanin. The OH stretching band for water adsorbed in synthetic L-Dopa melanin appears large, peaking at lower wavenumber values compared with the same band recorded for *Sepia* melanin ($\nu_{MAX} \approx 3420$ cm^{-1}) and submerging a weak shoulder at ~3200 cm^{-1}. By analogy to the analysis performed on *Sepia* melanin spectrum, the band was resolved

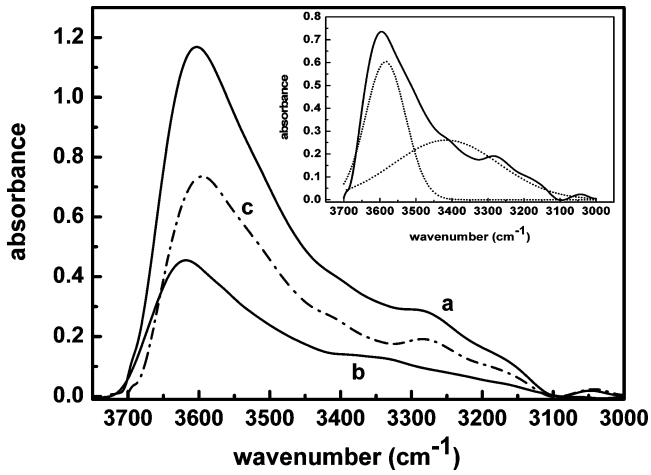

Figure 5. OH stretching band detected for *Sepia* melanin: (a) freshly prepared at $a_w = 0.92$ and (b) rehydrated at the same degree of hydration after a dehydration run up to $a_w = 0.06$. Curve c is the difference between curve a and curve b. In the inset: curve c is deconvoluted into two Gaussian components (dotted lines).

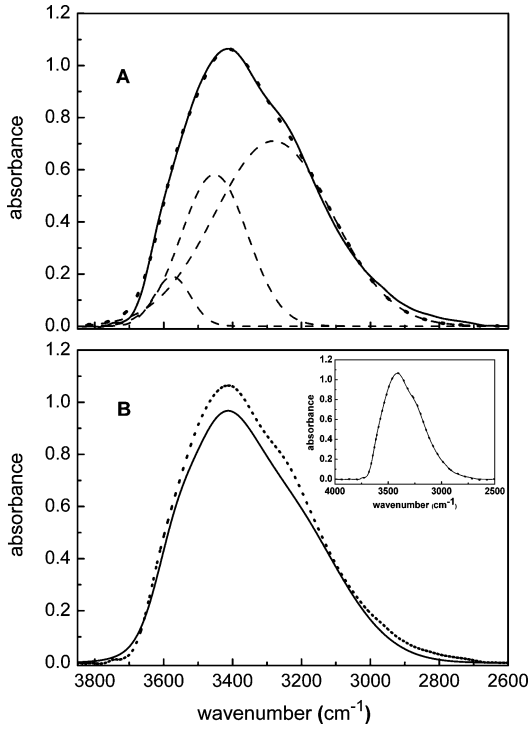

Figure 6. OH stretching bands measured for L-Dopa melanin. (A) Spectrum of the sample freshly prepared at $a_w = 0.92$ is decomposed into the three components obtained by Gaussian deconvolution of the band (dashed lines). The dotted line represents the sum of the components. (B) Comparison of the band of the sample freshly prepared (dotted line) and the band of the sample rehydrated at the initial a_w, after a dehydration run up to $a_w = 0.06$ (full line). In the inset, the two features are represented normalized to the maximum height: neither the band shape nor the position of the maximum is affected by the treatment.

into three Gaussian components, and Figure 6A shows the result of the decomposition performed on the band recorded at the highest a_w obtained ($a_w = 0.92$) in the HW ($\nu \approx 3575$ cm^{-1}), MW ($\nu \approx 3450$ cm^{-1}), and LW ($\nu \approx 3280$ cm^{-1}) bands.

Table 2 lists the corresponding H-bond distances, and all of the values are characteristic of hydration water in the liquid state.

The dehydration and rehydration processes were analyzed, as shown in Figure 7. The HW band shows a biphasic behavior

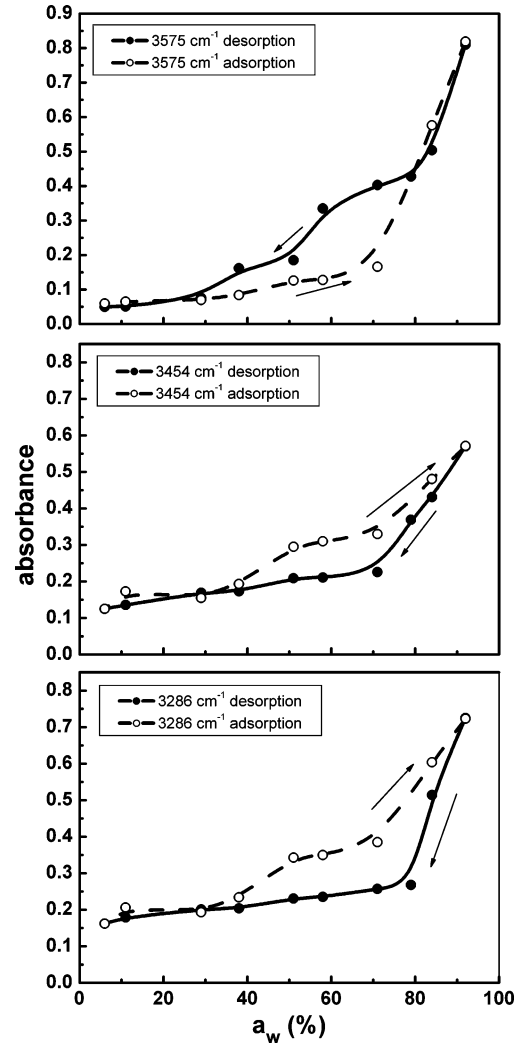

Figure 7. Desorption (●) and adsorption (○) data for L-Dopa melanin as deduced by the amplitudes of the three ν(OH) component bands (HW, MW, and LW) during the dehydration and hydration treatments. The lines are a guide for the eye.

during desorption (full symbols) showing an initial release of water up to $a_w = 0.79$, followed by a plateau and a successive water depletion for $a_w < 0.40$. MW and LW components show a different trend, both being characterized by a drastic reduction in amplitude for $0.92 < a_w < 0.70$. The peaks then attain a "saturation" value that is only slightly decreased by the subsequent dehydration treatments. The rehydration processes (empty symbols) reveal a pronounced hysteresis effect for the amplitude of all three bands. The HW adsorption plot exhibits a curve lying below the desorption curve displaying a slow initial rise up to $a_w = 0.70$, followed by a considerable increase in water uptake up to the final a_w value. For humidity values higher than $a_w = 0.80$, the two curves are coincident, and the final amplitude reaches the value detected in the original sample. MW and LW bands show the adsorption curves running above the desorption curves, suggesting that water molecules monitored by MW and LW bands could be easily readsorbed into the dry polymer. Although the isotherm curves do not superimpose, all three peaks recover the original amplitude at the end of the treatment. Figure 6B plots the band recorded for the sample at the start and at the end of the dehydration−hydration cycle. The amplitude of the band is almost completely gained at the end of the desorption−adsorption cycle, the difference in the areas of the two bands being <10%. In the inset of Figure 6B,

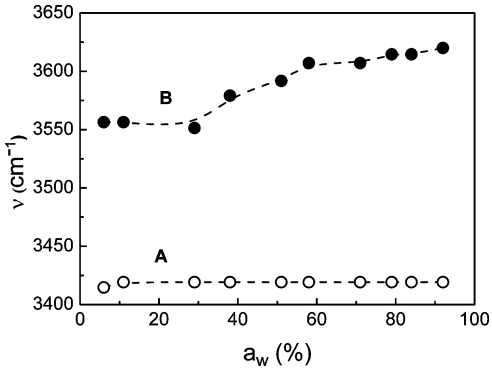

Figure 8. Changes in the position of the maximum of the overall ν(OH) band as a function of the water adsorbed (expressed as water vapor activity a_w) in (A) L-Dopa melanin (○) and (B) *Sepia* melanin (●). The lines are a guide for the eye.

we can observe the complete correspondence of the shapes of the two features, fully overlapping as normalized to the maximum height. In addition, it is worth noting that no band shift has occurred, either during desorption or during adsorption treatment, as shown in Figure 8A.

Analysis of the Adsorption Isotherms. The fitting procedure employed for the adsorption curves, tested in many cases on materials of technological interest and on foods, has the advantage of giving, through a proper selection of the parameters, direct insight into the structural and energy characteristics of the surface. However, a word of caution must be said regarding the straightforward application to melanin particles of models that are valid, for instance, on activated carbons. In fact, the differences in pore size distribution (PSD) and in the nature of surface chemical functionalities (representing putative primary adsorption centers) can play a profound role in the adsorption mechanism. Whereas materials such as activated carbon can be tailored with a wide range of porosity, melanins seem to present a limited porosity in the micropore region.[30]

PSD in melanin particles has been investigated by Eisenman et al. by means of NMR cryoporometry.[31] They were able to evaluate differences in the distribution of pore diameters between semisynthetic L-Dopa melanin incubated for 10 days on *Cryptococcus neoformans* and *Sepia* melanin, revealing a more pronounced porosity in the former.

To study the experimentally measured adsorption isotherms, some hypotheses as to the molecular models are necessary to analyze the shape of the curves.

At first glance, the graphs representing the water adsorption isotherms (Figure 9A,B) reveal two main differences: (1) Natural *Sepia* melanin shows isotherms of Type III (following the BDDT classification[24]), although the scale adopted and the presence of experimental errors cannot rule out some tendency toward a Type II behavior. (2) Synthetic melanin exhibits more complex isotherms not referable to any single adsorption mechanism. In other words, different mechanisms must be hypothesized in the different parts of the adsorption curve.
[24]

These preliminary observations suggest a profoundly different surface topography in the two kinds of particle.

In the case of natural melanin, we performed our study based on two multilayer adsorption models: the BET (Brunauer, Emmett, and Teller) theory, extended to the GAB (Guggenheim, Anderson, and de Boer) equation, and the Dubinin−Serpinski (D−S) model. The fitting of the data with these equations allows us to evaluate useful experimental parameters, listed in Table 3, to correlate with physical (and biophysical) properties.

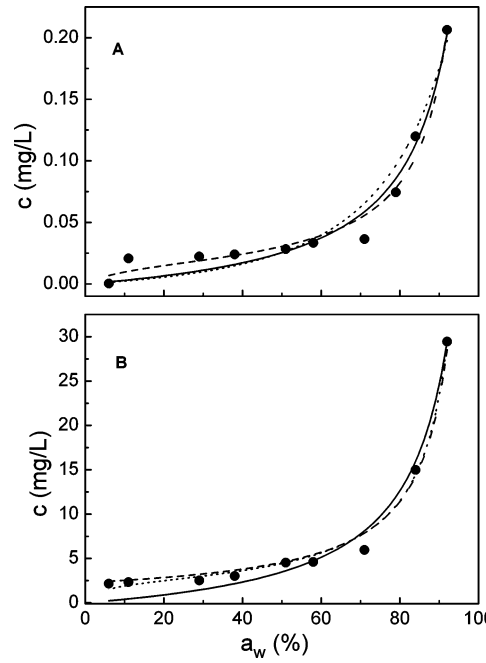

Figure 9. Adsorption isotherms as deduced by the amplitude of the component band at (A) 3350 cm^{-1} for *Sepia* melanin and at (B) 3575 cm^{-1} for L-Dopa melanin. Experimental points are shown (●). The lines represent the theoretical curves predicted by the GAB (•••), BET (---), and DS (—) models.

TABLE 3: Characteristic Values for Water Adsorption on *Sepia* Melanin Colloidal Particles

	parameters	3350 cm^{-1}	3550 cm^{-1}	3624 cm^{-1}
BET	n_m	0.017		0.004
	C	9.634		783.17
	R^2	0.976		0.972
GAB	n_m	0.249	0.513	
	C	0.100	0.277	
	K	0.795	0.645	
	R^2	0.943	0.930	
D−S	n_m	0.028	0.150	0.010
	J	0.957	0.768	0.894
	R^2	0.966	0.938	0.928

Discussion

In considering the experimental results, we started from the recently proposed model of melanin, that is, assuming for the melanin protomolecule a model consisting of a more or less irregular stacking of graphite-like plates.[6] The study presents a two-fold face. The hydration structure that was the object of the investigation was in fact suitable for capturing structural features of melanin by using water molecules as probes to assess the porosity of the adsorbent matrix. In the recent past, some model compounds have been employed to study the adsorption by melanin of simple fluids such as nitrogen, charged ions, and more complex adsorbates such as drugs.[25,32−35] The adsorption of water is, however, very different, because of the peculiar nature of this fluid, water molecules having the propensity to form H bonds that can be established both with other water molecules and with hydrophilic groups available on the polymer surface. We can hypothesize that water embedding melanin could seep into the granule, the surface of which is irregular and porous. A wide range of pores of different sizes and shapes can be envisaged where water molecules can be hosted. The wide variety of adsorption sites corresponds to the wide distribution of H_2O binding energies and accounts for the broadness of the IR bands measured. We can divide these sites

into two main categories: (1) the slits between the graphite walls of the protomolecules in which COOH and C═O groups are faced in different amount and differently arranged depending on the chemical nature of the melanin and (2) the interstices among the lamellar protomolecules. As concerns type 1 sites, as discussed in numerous papers studying water adsorption on activated carbon,[14,36,37] the layered structures provide pores represented by interlayer spaces where water molecules can be placed. It is reasonable to suppose that pores of small width, corresponding to small interlayer distances, host isolated water molecules that are attracted by the favorable chemical groups offered by the polymer wall but confined in a 2D region and cannot form with other water molecules the tetrahedral hydrogen-bonded network characteristic of the liquid state. In the infrared spectrum, they are responsible for the vapor-like typical absorption frequencies (*Sepia* melanin HW component). In larger pores, however, water can be filled and layered at bulk density and absorbs at relatively lower frequencies (liquid water absorption bands). Nevertheless, protomolecules aggregate to form the granule in assemblies holding interstitial voids (type 2 sites), heterogeneous in shape and width and randomly arranged in the nanogranule, where water can be included. The lateral extension of the protomolecules in the two types of melanin suggests that in both of the materials, the dimensions of such crevices, although different in size and shape, can collect the water that is responsible for the LW component band in both melanin spectra, which broadness, however, could also be due to the contribution of some vibrational modes of the liquid fraction included in the largest lamellar structure of the protomolecules. This fact explains the LW component spreading over the frequencies typical for water in the liquid phase.

On the basis of the experimental results, a model describing the adsorption−desorption kinetic of water in the two melanins can be tentatively proposed.

In the hydrated state, *Sepia* melanin hosts both free water molecules behaving as in the vapor state in the narrowest graphitic wall space (HW component) and water in the liquid phase in the larger interlayer pores (MW component). The hydrogen bond distances corresponding to the former component (Table 2) are typical for straight hydrogen bonding. They are suggestive for individual water molecules connecting, as bridges, opposing walls of these small pores. They are singly adsorbed on the available surface sites (carboxylic, hydroxyl, phenolic groups) decorating the graphitic pore surface and can act, where the interlayer distances allow, as nuclei for the formation of water clusters responsible for the MW component. The MW peak amplitude and position are strongly dependent on the cluster sizes, and their changes allow us to monitor the mechanism of water inclusion and extrusion. Where the interlayer distances are large, large water clusters of liquid-like density form, whereas in the smaller ones, there is considerable empty space. The more red-shifted band (i.e., the LW component) appears considerably broader than the other features and can be attributed to stretching vibrations of the OH groups engaged in hydrogen bonds typical of bulk water. We hypothesize that this band may represent the peak deriving from the water embedded in the crevices among and around the protomolecules because this water has the structural and dynamic properties of free liquid water.

By changing the hydration level, the spectrum evolves and exhibits hysteresis effects. The behavior of MW and LW component bands, which are related to the liquid water fraction, during the desorption phase reflects the depletion of the pores and cavities available to lodge liquid water. At the lowest relative water pressure, when liquid water has emptied from the polymer pores, it is a well-founded supposition that bridges between opposing H-bonding available groups could be formed without the intervention of water molecules. The establishment of such links could induce shrinkage of the molecular structure and the collapse of the polymer structure at some point. Residual water molecules included in the restricted matrix cavities, being in a closer available space, will be characterized by shorter hydrogen bond distances. This effect might be responsible for the reduced amplitude, the red shift, and the change in the reciprocal ratio of the component bands detected in the spectral feature of the dehydrated sample (Figure 3). Water molecules in vapor phase, contributing to the HW feature, are also desorbed, as confirmed by the decrease in amplitude.

The structural rearrangement in the polymer matrix as a consequence of the dehydration produces a restriction in water readsorption during the rehydration treatment. Water adsorption, both in the gaseous and in the liquid phases, at first induces a swelling of the layered structures, as shown by the blue shift undergone by the IR absorption bands during the initial phases of the process, and this can favor the adsorption both of single molecules and of the liquid fraction, albeit in different proportions. The storage of single H_2O molecules, in fact, is facilitated, because of their small size compared with water clusters, as can be inferred by inspecting Figure 4, where the adsorption isotherm curve of the HW band runs above the desorption curve. The further water depletion process is limited by the partial loss of flexibility and resistance to swelling of the matrix. As a result, a large amount of water in the liquid phase cannot be readsorbed The original band shape and amplitude cannot be completely recovered, even by restoring the initial degree of hydration, as demonstrated by the hysteresis effect monitored in Figure 5 and inset.

The picture of the synthetic melanin structure appears different from that of the natural structure. The L-Dopa melanin granule can be described as an aggregate of protomolecules with a lamellar structure as well but with a larger lateral extension and larger pores than those of natural melanin. In this type of melanin, water can be adsorbed only in liquid phase. (See Table 2.) The adsorption hysteresis monitored in the isotherms (Figure 7) does not mirror changes in the macromolecular architecture. We have excluded modifications in the polymer matrix, as in the natural compound, because adsorption and desorption runs do not induce a shift in the position of the absorption component bands (Figure 6). This fact allows us to rule out any shrinking of the macromolecule during the removal of water or swelling by restoring the solvent. Such a result could be interpreted either to the assumption that the pore walls are separated by a distance sufficient to avoid any possible interaction once empty or to the lack of chemical groups belonging to facing layers in the pores available to interact.

The results of the theoretical isotherm analysis support and help to clarify some points in the discussion above. They can be summarized as follows.

Natural *Sepia* melanin: the three peaks appear to correspond to different adsorption mechanisms. Table 3 summarizes the results and shows that the three theoretical models describe the experimental behavior with a considerable degree of confidence, as indicated by the values of R^2. (We have considered only values of parameters corresponding to $R^2 > 0.9$.) Some peculiarities should be noticed. First, the values of n_m are lower than those in the case of adsorption of water on other materials such as methylcellulose[25] and carbon.[27] Another interesting characteristic is the value of c, suggesting a Type II behavior,

and consequently justifying the BET analysis. More problematic is the meaning of the adsorption mechanisms that are at the base of the three IR peaks, in terms of both primary binding to hydrophilic groups and condensation of water clusters on this "first layer" of adsorbed water. On the basis of the values of the n_m parameters and on chemical evaluations of hydrophilic surface groups, we can suppose that the adsorption at 3624 cm^{-1} can be attributed to the adsorption of insulated water molecules.

Synthetic L-Dopa melanin: only the isotherm related to the peak at 3575 cm^{-1} can be analyzed because the fittings of the other curve with GAB equations provide n_m values that are totally unacceptable. The only conclusion we can draw is that there is a considerably higher affinity for water (as shown by the n_m values) and surface concentration of primary hydrophilic centers, comparable to that measured on activated carbon, as observed by Tsunoda et al.[38] by means of the D−S analysis.

Conclusions

In this article, we have presented a detailed and systematic analysis of water adsorption on melanin, natural from *Sepia* ink sac and synthetic from auto-oxidation of L-Dopa. We used FTIR spectroscopy to investigate the structural properties and the behavior of the bound water. The absorption OH stretching band and the water sorption isotherms deduced from the amplitude evolution of the ν(OH) component bands were also investigated. The two melanins appear structurally different, the different structures affecting their wettability.

The emerging models can be described as follows: (1) the nanogranular structure proposed for natural melanin accounts for assuming largely heterogeneous graphitic pores, small enough to lodge single water molecules, as in the vapor phase, and larger, where water in the liquid phase can be clustered. Its structure is flexible; therefore, the pore sizes are modified by the adsorption and desorption of water, although it shrinks irreversibly by the drastic removal of water, which induces the chemical interaction between functionalities located on the opposite walls. (2) Synthetic L-Dopa melanin appears as a "simpler" system characterized by a more uniform size of the interlayer spacing between pore walls, where water can be adsorbed in the liquid form, and is stiff enough to avoid deformations as a consequence of dehydration−rehydration treatments. It exhibits a large affinity for the water that fills all available cavities in the liquid phase.

The presence of liquid water molecules showing the bulk water properties can be hypothesized for both melanin types. It embeds the crevices among the protomolecules in the granules, differing in size and shape, but definitely larger in the synthetic melanin, which is characterized by assembling structures with a larger lateral surface extension. This fact could account for the difficulty encountered in finding a theoretical model to describe the water desorption in this compound completely, which might have an uncharacteristic mode of water sorption, and for the higher amount of water adsorbed. In *Sepia* melanin, a condensation mechanism for water included in the intraprotomolecule cavities can be inferred.

Melanin, as an adsorbent material, therefore appears to be a very complex system, heterogeneous in chemical composition and characterized by a high pore size dispersity where water can be included in differing aggregation states. In this light, the terms "bound" and "free" water employed in past papers assume a different meaning. More realistically, they can be related, respectively, to the gaseous phase of water that is retained in the smaller pores even under extreme dehydration conditions and to the hydrogen-bonded liquid or liquid-like fraction, which, accumulating in large pores and crevices, can be easily adsorbed and desorbed. The differing interaction exhibited by the different melanins with water could account for the modulation of their solubility in water and for the differences in their color shades.

References and Notes

(1) Nicolaus, R. A. *Melanins*; Hermann: Paris, 1968.

(2) Prota, G. *Melanins and Melanogenesis*; Academic Press: San Diego, 1992.

(3) Crippa, P. R.; Hjorak, V.; Prota, G.; Svoronos, P.; Wolfram, L. *The Alkaloids*; Academic Press: New York, 1989; Vol. 366, pp 253−322.

(4) Clancy, C. M. R.; Simon, J. D. Ultrastructural organization of eumelanin from *Sepia officinalis* measured by atomic force microscopy. *Biochemistry* **2001**, *40*, 13353–13360.

(5) Thathachari, Y. T.; Blois, M. S. Physical Studies on melanin II. X-ray diffraction. *Biophys. J.* **1969**, *9*, 77–89.

(6) Cheng, J.; Moss, S. C.; Eisner, M. X-ray characterization of melanin- II. *Pigm. Cell Res.* **1994**, *7*, 263–273.

(7) Bardani, L.; Bridelli, M. G.; Carbucicchio, M.; Crippa, P. R. Comparative Mössbauer and infrared analysis of iron-containing melanins. *Biochim. Biophys. Acta* **1982**, *716*, 8–15.

(8) Zajac, G. W.; Gallas, G. M.; Cheng, J.; Eisner, M.; Moss, S. C.; Alvarado-Swaisgood, A. E. The fundamental unit of synthetic melanin: a verification by tunneling microscopy of X-ray scattering results. *Biochim. Biophys. Acta* **1994**, *1199*, 271–278.

(9) Kaxiras, E.; Tsolakidis, A.; Zonios, G.; Meng, S. Structural model of eumelanin. *Phys. Rev. Lett.* **2006**, *97*, 218102–218104.

(10) D'Ischia, M.; Napolitano, A.; Pezzella, A.; Land, E. J.; Ramsden, C. A.; Riley, P. A. 5,6-Dihydroxyindoles and indole-5,6-diones. *Adv. Heterocycl. Chem.* **2005**, *289*, 1–63.

(11) Albanese, G.; Bridelli, M. G.; Deriu, A. Structural dynamics of melanin investigated by Rayleigh scattering of Mössbauer radiation. *Biopolymers* **1983**, *23*, 1481–1498.

(12) Meredith, P; Sarna, T. The physical and chemical properties of eumelanin. *Pigment Cell Res.* **2006**, *19*, 572–594.

(13) Striolo, A.; Chialvo, A. A.; Cummings, P. T.; Gubbins, K. E. Water adsorption in carbon-slit nanopores. *Langmuir* **2003**, *19*, 8583–8591.

(14) Jorge, M.; Schumacher, C.; Seaton, N. A. Simulation studies of the effect of the chemical heterogeneity of activated carbon on water adsorption. *Langmuir* **2002**, *18*, 9296–9306.

(15) Gelb, L. D.; Gubbins, K. E.; Radhakrishnan, R.; Sliwinska-Bartkowiak, M. Phase separation in confined systems. *Rep. Prog. Phys.* **1999**, *62*, 1573–1659.

(16) Striolo, A.; Gubbins, K. E.; Chialvo, A. A.; Cummings, P. T. Simulated water adsorption isotherms in carbon nanopores. *Mol. Phys.* **2004**, *102*, 243–251.

(17) Brennan, J. K.; Bandosz, T. J.; Thomson, K. T.; Gubbins, K. E. Water in porous carbons. *Colloids Surf., A* **2001**, *187−188*, 539–568.

(18) Bridelli, M. G.; Capelletti, R.; Crippa, P. R. Infrared spectroscopy of eye and synthetic melanins at various values of pH and hydration. *Physiol. Chem. Phys.* **1980**, *12*, 233–240.

(19) Bridelli, M. G.; Tampellini, D.; Zecca, L. The structure of neuromelanin and its iron binding sites studied by infrared spectroscopy. *FEBS Lett.* **1999**, *457*, 18–22.

(20) Ping, Z. H.; Nguyen, Q. T.; Chen, S. M.; Zhou, J. Q.; Ding, Y. D. States of water in different hydrophilic polymers-DSC and FTIR studies. *Polymer* **2001**, *42*, 8461–8467.

(21) Mallamace, F.; Chen, S. H.; Broccio, M.; Corsaro, C.; Crupi, V.; Majolino, D.; Venuti, V.; Baglioni, P.; Fratini, E.; Vannucci, C.; Stanley, H. E. Role of the solvent in the dinamica transitions of proteins: the case of the lysozyme-water system. *J. Chem. Phys.* **2007**, *127*, 045104−1.

(22) Venyaminov, S. Yu.; Prendergast, F. G. Water (H_2O and D_2O) molar absorptivity in the 1000−4000 cm^{-1} range and quantitative infrared spectroscopy of aqueous solutions. *Anal. Biochem.* **1997**, *248*, 234.

(23) Bertie, J. E.; Lan, Z. Infrared intensities of liquids XX: the intensity of the OH stretching band of liquid water revisited, and the best current values of the optical constants of H_2O(l)at 25°C between 15,000 and 1 cm^{-1}. *Appl. Spectrosc.* **1996**, *50*, 1047–1057.

(24) Gregg, S. J.; Sing, K. S. W *Adsorption, Surface Area, and Porosity*; Academic Press: New York, 1982.

(25) Velasquez, G.; Herrera-Gómez, A.; Martín-Polo, M. O. Theoretical determination of first adsorbed layer of water in methylcellulose. *J. Food Eng.* **2003**, *59*, 45–50.

(26) Gauden, P. A. Does the Dubinin−Serpinsky theory adequately describe water adsorption on adsorbents with high-energy centers? *J. Colloid Interface Sci.* **2005**, *282*, 249–260.

(27) Rutherford, S. W. Modeling water adsorption in carbon micropores: study of water in carbon molecular sieves. *Langmuir* **2006**, *22*, 702–708.

(28) Clough, A.; Kneizys, F. X.; Davies, R.; Gamache, R.; Tipping, R. *Atmospheric Water Vapor*; Academic Press: New York, 1980.

(29) Nakamoto, K.; Margoshes, M.; Rundle, R. E. Stretching frequencies as a function of distances in hydrogen bonds. *J. Am. Chem. Soc.* **1955**, *77*, 6480–6486.

(30) Crippa, P. R.; Giorcelli, C.; Zeise, L. Determination of surface characteristics and fractal dimensions of natural and synthetic eumelanins from nitrogen adsorption isotherms. *Langmuir* **2003**, *19*, 348–353.

(31) Eisenman, H. C.; Nosanchuk, J. D.; Beau, J.; Webber, W.; Emerson, R. J.; Camesano, T. A.; Casadevall, A. Microstructure of cell wall-associated melanin in the human pathogenic fungus *Cryptococcus neoformans*. *Biochemistry* **2005**, *44*, 3683–3693.

(32) Dastgheib, S. A.; Rockstraw, D. A. A model for the adsorption for single metal ion solutes in aqueous solution onto activated carbon produced from pecan shells. *Carbon* **2002**, *40*, 1843–1851.

(33) McKay, G., III. *J. Chem. Technol. Biotechnol.* **1983**, *33A*, 196–204.

(34) Bridelli, M. G.; Ciati, A.; Crippa, P. R. Binding of chemicals to melanin re-examined: adsorption of some drugs to the surface of melanin particles. *Biophys. Chem.* **2005**, *118*, 121–129.

(35) Bridelli, M. G.; Crippa, P. R. Theoretical analysis of the adsorption of metal ions to the surface of melanin particles. *Adsorption* **2008**, *14*, 101–109.

(36) McCallum, C. M.; Bandosz, T. J.; McGrother, S. C.; Müller, E. A.; Gubbins, K. E. A molecular model for adsorption of water on activated carbon: comparison of simulation and experiment. *Langmuir* **1999**, *15*, 533–544.

(37) Salame, I. I.; Bandosz, T. J. Experimental study of water adsorption on activated carbons. *Langmuir* **1999**, *15*, 587–593.

(38) Tsunoda, R.; Ozawa, T.; Ando, J. Ozone treatment of coal- and coffee grounds-based active carbons: water vapor adsorption and surface fractal micropore. *J. Colloid Interface Sci.* **1998**, *205*, 265–270.

JP101833K